Siberian Branch of Russian Academy of Science
BUDKER INSTITUTE OF NUCLEAR PHYSICS

R.R.Akhmetshin, G.A.Aksenov, E.V.Anashkin,
M.Arpagaus, B.O.Baibusinov, V.S.Banzarov,
L.M.Barkov, A.E.Bondar, D.H.Brown, D.V.Chernyak,
V.V.Danilov, A.S.Dvoretsky, S.I.Eidelman,
G.V.Fedotovich, N.I.Gabyshev, A.A.Grebeniuk,
D.N.Grigoriev, V.W.Hughes, P.M.Ivanov, B.I.Khazin,
I.A.Koop, L.M.Kurdadze, A.S.Kuzmin, I.B.Logashenko,
P.A.Lukin, Yu.I.Merzlyakov, I.N.Nesterenko,
V.S.Okhapkin, A.A.Polunin, V.I.Ptitzyn, T.A.Purlatz,
B.L.Roberts, N.I.Root, A.A.Ruban, N.M.Ryskulov,
A.G.Shamov, Yu.M.Shatunov, B.A.Shwartz,
V.A.Sidorov, A.N.Skrinsky, V.P.Smakhtin, I.G.Snopkov,
E.P.Solodov, P.Yu.Stepanov, A.I.Sukhanov, V.M.Titov,
J.A.Thompson, Yu.V.Yudin, S.G.Zverev

STUDY OF DYNAMICS OF $\phi \to \pi^+\pi^-\pi^0$ DECAY WITH CMD-2 DETECTOR

Budker INP 98-30

http://www.inp.nsk.su/publications

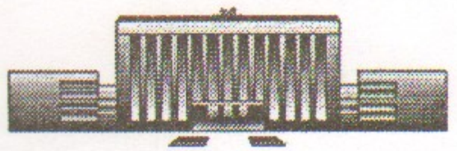

Novosibirsk
1998

Study of dynamics of $\phi \to \pi^+\pi^-\pi^0$ decay with CMD-2 detector

R.R.Akhmetshin, G.A.Aksenov, E.V.Anashkin, M.Arpagaus, B.O.Baibusinov, V.S.Banzarov, L.M.Barkov, A.E.Bondar, D.V.Chernyak, V.V.Danilov, A.S.Dvoretsky, S.I.Eidelman, G.V.Fedotovich, N.I.Gabyshev, A.A.Grebeniuk, D.N.Grigoriev, P.M.Ivanov, B.I.Khazin, I.A.Koop, L.M.Kurdadze, A.S.Kuzmin, I.B.Logashenko, P.A.Lukin, Yu.I.Merzlyakov, I.N.Nesterenko, V.S.Okhapkin, A.A.Polunin, V.I.Ptitzyn, T.A.Purlatz, N.I.Root, A.A.Ruban, N.M.Ryskulov, A.G.Shamov, Yu.M.Shatunov, B.A.Shwartz, V.A.Sidorov, A.N.Skrinsky, V.P.Smakhtin, I.G.Snopkov, E.P.Solodov, P.Yu.Stepanov, A.I.Sukhanov, V.M.Titov, Yu.V.Yudin, S.G.Zverev.*

Budker Institute of Nuclear Physics
630090 Novosibirsk, Russia

D.H.Brown, B.L.Roberts

Boston University, Boston, MA 02215, USA

J.A.Thompson

University of Pittsburgh, Pittsburgh, PA 15260, USA

V.W.Hughes

Yale University, New Haven, CT 06511, USA

Abstract

A study of the $\phi \to \pi^+\pi^-\pi^0$ decay mode has been performed using a data sample of about 2.0 million ϕ decays collected by the CMD-2 detector at VEPP-2M collider in Novosibirsk. The following parameters of the ϕ-meson have been measured: $Br(\phi \to \pi^+\pi^-\pi^0) = 0.145 \pm 0.009 \pm 0.003$ and $\delta_{\phi-\omega} = 162 \pm 17°$. The analysis of the Dalitz plot showed the dominance of the $\phi \to \rho\pi$ intermediate mechanism, the limits for the ratio of the direct amplitude of $\phi \to 3\pi$ to that of $\phi \to \rho\pi$ are $-0.16 < a_1 < 0.11$ at 90% C.L. The upper limits for the probabilities of the decay modes $\phi \to \pi^+\pi^-\eta$ and direct $\phi \to \rho\gamma\gamma$ have been found for the first time: $Br(\phi \to \pi^+\pi^-\eta) < 3 \times 10^{-4}$ and $Br(\phi \to \rho\gamma\gamma) < 5 \times 10^{-4}$ at 90% C.L.

*Deceased

1 Introduction

$\phi \to 3\pi$ decay is one of the dominant decay modes of the ϕ-meson despite the OZI rule suppression. Precise measurements of its parameters provide valuable information for physics of light quarks. In addition, the cross section of the reaction $e^+e^- \to \omega(\phi) \to 3\pi$ gives a significant contribution to the total hadronic cross section and therefore to the accuracy of muon $(g-2)_\mu$ and $\alpha(M_Z^2)$ calculations.

The branching ratio for the $e^+e^- \to \phi \to 3\pi$ decay mode has been earlier measured by different groups in Orsay [1, 2, 3] and Novosibirsk [4, 5, 6]. The Dalitz plot analysis of the 3π final state was performed in one experiment [7] only which gave evidence for the dominance of the $\phi \to \rho\pi \to 3\pi$ mechanism of this decay despite a restricted data sample.

Since 1992 the CMD-2 detector [8, 9] has been running at the high luminosity collider VEPP-2M [10]. CMD-2 combines a magnetic spectrometer for charged particles [11] and an electromagnetic calorimeter [12] with high efficiency and good resolution for photons to study vector meson decays with high accuracy as well as to search for rare processes. First results from the CMD-2 detector were published in [13], a study of the four major modes of the ϕ-meson decay.

This paper presents branching ratio and Dalitz plot studies of the $\pi^+\pi^-\pi^0$ mode of the ϕ-meson decay. The analysis is based on the data sample corresponding to the production of about $2.0 \times 10^6 \phi$'s, a factor of 5 bigger compared to that in [13].

The total amplitude of the $\phi \to 3\pi$ decay is taken to be a linear combination of the $\phi \to \rho\pi \to 3\pi$ and contact $\phi \to \pi^+\pi^-\pi^0$ term. Results on their

contributions are presented in terms of the ratio of the amplitudes. Because of the strong interference between the two amplitudes it is meaningless to quote the corresponding branching ratios separately.

We have also placed an upper limit for the direct decay $\phi \to \rho\gamma\gamma$ in the case when two photons are coming neither from the π^0 decay nor from the decay $\phi \to \eta\gamma$ followed by the $\eta \to \pi^+\pi^-\gamma$. An upper limit is given for the G-parity suppressed decay mode $\phi \to \eta\pi^+\pi^-$.

The CMD-2 Detector

The CMD-2 detector has been described in detail elsewhere [8, 9]. It is a general purpose detector consisting of a drift chamber(DC) with about 250 μ resolution transverse to the beam and proportional Z-chamber used for the trigger, both inside a thin (0.4 X_0) superconducting solenoid with a field of 1 T.

The barrel calorimeter placed outside of the solenoid consists of 892 CsI crystals of 6×6×15 cm^3 size and covers polar angles from 0.8 to 2.3 radian. The energy resolution for photons in the CsI calorimeter is about 9% in the energy range from 50 up to 600 MeV. The BGO endcap calorimeter was not yet installed when the data sample presented here was taken.

The muon system is composed of two layers of streamer tubes separated by the 15 cm thick iron magnet yoke. Its spatial resolution is about 2.5 cm.

The trigger signal is generated either by the Trackfinder based on the DC and Z-chamber hits [14] or by the neutral trigger which takes into account the number of clusters detected in the CsI calorimeter as well as the total energy deposition. The integrated luminosity of 1425 nb^{-1} collected at 14 energy points around the ϕ-meson mass corresponds to the production of about $2.0 \times 10^6 \phi$'s. In total, the processed data sample contains about 7.2×10^7 events.

Selection of $\pi^+\pi^-\pi^0$ events

The present analysis is based on completely reconstructed 3π events. At the initial stage, events with one positive and one negative charged particle and two or more reconstructed photon clusters were selected. Then the following criteria were applied:

- All charged particles and photons are required to hit the detector within the solid angle limited by the polar angle $|\theta - \frac{\pi}{2}| < 0.67$ radians to avoid edge effects for the detection efficiency;
- For charged particles:
  - The distance from each track to the beam axis should be $R_{min} < 0.3\ cm$ in the $(R-\varphi)$ projection and the distance from a track to the interaction point along the beam direction should be $|Z_{tr}| < 10\ cm$;
  - The momentum corresponding to each track is required to be $P_\pi > 130\ MeV/c$ to reject charged kaons and $P_\pi < 500\ MeV/c$ to suppress the cosmic background;
- For the neutral pion:
  - The invariant mass of two photons must be in the range $90\ MeV/c^2 < m_{\gamma\gamma} < 160\ MeV/c^2$. If more than two showers are detected, the kinematic reconstruction for each pair is carried out assuming the 3π decay, and the pair with the best χ^2 is selected;
  - The energy of each photon $E_{\gamma,i}$ should be larger than 30 MeV;
- Missing mass of each meson pair $m^2_{miss:i,j} = (P_\phi - P_i - P_j)^2$ corresponds to the pion mass: $|\frac{m^2_{miss:i,j}}{m^2_\pi} - 1| < 5$, where P_ϕ, P_i are four-momenta of the ϕ- and i-th π-meson respectively.

With the above criteria, 11169 events were selected in total.

The distributions in the two photon invariant mass and Z-coordinate of the charged particle vertex for selected events are shown in Fig. 1.

The background for this decay mode can originate from true e^+e^- interactions or from cosmic particles and beam interactions with the residual gas.

The main processes which can imitate 3π events are the following:

- $e^+e^- \to \pi^+\pi^-\pi^0\pi^0$;
- $e^+e^- \to \phi \to \eta\gamma$, $\eta \to \pi^+\pi^-\pi^0$ or $\pi^+\pi^-\gamma$;
- $e^+e^- \to \phi \to K_L K_S$ or K^+K^-;
- $e^+e^- \to e^+e^-\gamma\gamma$, $e^+e^- \to \pi^+\pi^-\gamma\gamma$, and $e^+e^- \to \pi^+\pi^-\gamma$, where for the last process the second required cluster is produced by a pion nuclear shower;

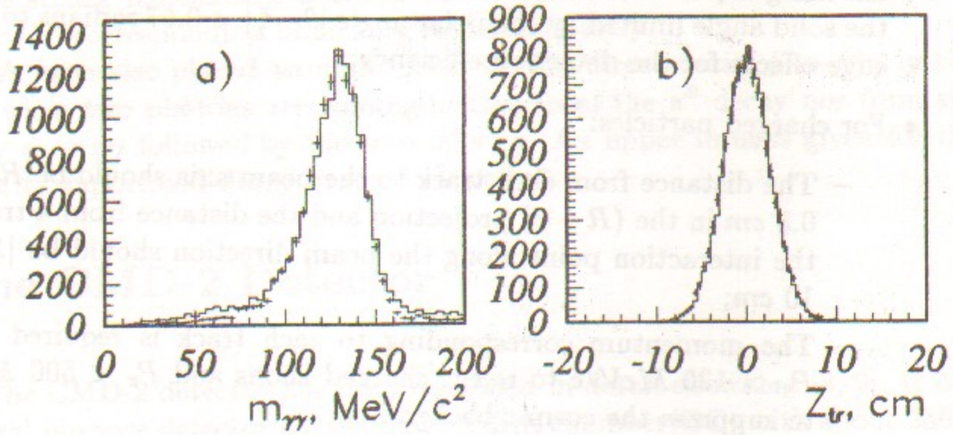

Figure 1: Distributions for selected events: a) – two photon invariant mass; b) – Z-vertex coordinate. Solid line – selected events; crosses – Monte Carlo simulation of $e^+e^- \to \pi^+\pi^-\pi^0$.

- Cosmic particles and beam interaction with the residual gas.

The contribution of the first two processes was calculated using the experimental data for the cross sections [6, 15] and the detection efficiency from Monte Carlo simulation.

To study the background from $e^+e^- \to e^+e^-\gamma\gamma$, events from this process were specially selected by the requirements that the energy deposition in CsI corresponding to the charged particle $E_{ch,i}$ should be close to its measured momentum P_i: $|E_{ch,i}/P_i - 1| < 0.2$.

According to the simulation, about $73 \pm 3\%$ of $e^+e^-\gamma\gamma$ events and $1.1 \pm 0.2\%$ of 3π events satisfy this selection. Using energy points beyond the ϕ region where the contribution of 3π is negligible, the number of events of $e^+e^- \to e^+e^-\gamma\gamma$ was found and, assuming the $1/E^2$ cross section behaviour, this background contribution was estimated for each energy point.

To estimate the $\pi^+\pi^-\gamma\gamma$, $\pi^+\pi^-\gamma$ background contamination arising from a radiative correction to the process $e^+e^- \to \pi^+\pi^-$, the ratio between $\pi^+\pi^-\gamma\gamma$ and $e^+e^-\gamma\gamma$ events was determined for the cases in which two photons do not form a π^0 : $m_{\gamma\gamma} < 50\ MeV/c^2$ or $m_{\gamma\gamma} > 170\ MeV/c^2$. Assuming this ratio to be the same for the region $90 < m_{\gamma\gamma} < 160\ MeV/c^2$, the number of the background events was calculated.

Background from cosmics and beam interactions was found by applying the event selection criteria to events with Z between 10 and 20 cm, away from the interaction point.

The $K\bar{K}$ background appears because of the incorrect reconstruction caused by kaon decays or nuclear interactions. Such events have the wide distribution both over m_{miss} and R_{min}. This background source is particularly important because of its resonant nature. Its contribution was calculated from the number of events detected in the region of the missing mass outside the π mass: $5 < |\frac{m^2_{miss:i,j}}{m^2_\pi} - 1| < 10$. The ratio of the number of background events in the main missing mass region and the region above was measured based on the events with $R_{min} > 0.4$ cm.

The total numbers of the selected 3π and background events are presented in Table 1. The shown error of the 3π event number includes both statistical uncertainty and accuracy of subtracted background.

Table 1: Statistics of the selected events of 3π and the background processes.

$\int Ldt$	$N_{selected}$	$N_{3\pi}$	$N_{4\pi}$	$N_{\eta\gamma}$	$N_{ee\gamma\gamma+\pi\pi\gamma\gamma}$	$N_{K\bar{K}}$	$N_{cosm+beam}$
1425 nb^{-1}	11169	10794 ± 114	92 ± 9	10 ± 2	113 ± 39	153 ± 27	7 ± 3

Detection efficiency calculation

The cross section at each energy point was calculated according to the formula:

$$\sigma_{3\pi} = \frac{N_{3\pi}}{L\varepsilon_{trig}\varepsilon_{MC}(1-\delta_{MC})(1+\delta_{rad})(1+\delta_{wid})}, \quad (1)$$

where L is the integrated luminosity determined from the detected number of the collinear e^+e^-, $\mu^+\mu^-$ and $\pi^+\pi^-$ events; ε_{MC} is the detection efficiency calculated from Monte Carlo simulation; ε_{trig} is a trigger efficiency; δ_{MC} is a correction for the effects not taken into account by the simulation; δ_{rad} is a radiative correction; δ_{wid} is a correction for the beam spread.

Since trigger signals were produced both by the Trackfinder and calorimeter the trigger efficiency can be determined for each case by the selection of the events triggered by the alternative source. The final value of the trigger efficiency was found to be $\varepsilon_{trig} = 99.6 \pm 0.4\%$.

Monte Carlo simulation of the detector is based on the GEANT code. The detection efficiency for 3π events for our selection criteria was found to be $\varepsilon_{MC} = 4.93\%$ for an ideal detector. However our Monte Carlo simulation doesn't describe correctly the nuclear interaction of low energy hadrons. There were also some apparatus effects in the experimental runs of 1993 such as the gain and ionization absorption instability in the DC as well as few dead electronics channels in DC and CsI calorimeter which could affect the detection efficiency but weren't taken into account in Monte Carlo. To estimate the correction for these effects, δ_{MC}, a special study was performed.

Assuming that the reconstruction efficiency for each particle is uncorrelated with the others, this factor $(1-\delta_{MC})$ can be presented as

$$(1-\delta_{MC}) = \varepsilon_+\varepsilon_-\varepsilon_0 \ , \qquad (2)$$

where ε_i is the ratio of the real reconstruction efficiency of the i–th pion to that predicted by Monte Carlo. To determine ε_i the events of 3 classes were analyzed, each containing at least 2 particles ($\pi^+\pi^-$, $\pi^+\pi^0$ or $\pi^-\pi^0$) without taking into account the third one. Such events can be completely reconstructed by using parameters of two particles and four-momentum conservation. For each class of events the efficiency $\varepsilon_{rec\ 2}$ can be written as

$$\varepsilon_{rec\ 2} = \varepsilon_i\varepsilon_j \ . \qquad (3)$$

From (2) and (3) all ε_i can be calculated separately and the value of δ_{MC} is determined as well. The background for these three classes is higher than for the case when all particles are detected. Thus, by this method we could determine the efficiency with reasonable accuracy only for seven energy points near the top of the ϕ peak. The efficiency for other points was assumed to be equal to its average value. The quoted errors include the rms spread over the averaged points.

The radiative correction to the Born cross section $e^+e^- \to 3\pi$ took into account the processes when in addition to 3π the final state contains one or several low energy photons which are emitted mainly close to the beam direction. Such events are still identified as 3π events due to imperfect reconstruction. The visible cross section can be written according to [16] as

$$\sigma_{vis}(s) = \int_0^1 \sigma_0\Big(s(1-x_+)(1-x_-)\Big)D(x_+)D(x_-)\epsilon(x_+x_-)dx_+dx_-, \qquad (4)$$

where $\sigma_0(s)$ and $\sigma_{vis}(s)$ are Born and visible cross sections respectively, $D(x)$ is a function of the fraction of energy x taken by emitted photons calculated in [16]. Here x_+, x_- refer to initial electron and positron respectively,

$\epsilon(x_+, x_-)$ is an efficiency to detect the $3\pi\gamma(\gamma)$ system as 3π which is calculated using Monte Carlo. The effect of radiative corrections is usually small and can be expressed as a factor $(1+\delta_{rad}(s))$:

$$\sigma_{vis}(s) = \sigma_0(s)(1+\delta_{rad}(s)), \qquad (5)$$

which is calculated by the iterative procedure using the energy dependence of the cross section according to (4). For the last two energy points $\sigma_0(s) \ll \sigma_{vis}(s)$ and the obtained $\delta_{rad}(s)$ is a big factor. This results in decreasing accuracy for $\sigma_0(s)$ determination.

The beam energy spread for this experiment was $\sigma_E = 0.30\ MeV$. The visible cross section is the convolution of the true cross section with the beam energy distribution and is taken into account by the factor δ_{wid}.

The values of the luminosity, efficiency and corrections discussed above as well as the number of events and experimental value of the cross section for each energy point are presented in Table 2. The energy of the collider was set roughly by the dipole magnet current. A more precise determination of the beam energy was made using the measurement of the average momentum of the charged kaons in the $e^+e^- \to \phi \to K^+K^-$ reaction [13]. The energy errors shown in Table 2 include the statistical uncertainty as well as the point-to-point energy accuracy. The uncertainty of the absolute energy determination was 0.1 MeV.

ϕ-meson parameters

The cross section of $e^+e^- \to 3\pi$ was parametrized by a sum of three interfering amplitudes – ϕ and ω mesons with some constant background.

$$\sigma_{3\pi}(s) = \frac{F_{3\pi}(s)}{s}\cdot|A_\omega + A_\phi e^{i\delta_\phi} + A_{bg}|^2, \qquad (6)$$

$$A_V = \frac{m_V^2\Gamma_V\sqrt{\sigma_V/F_{3\pi}(m_V^2)}}{s - m_V^2 + i\sqrt{s}\Gamma_V(s)}, \qquad (7)$$

$$A_{bg} = m_\phi\sqrt{\sigma_{bg}/F_{3\pi}(m_\phi^2)}, \qquad (8)$$

where m_V, Γ_V, σ_V are mass, width and peak cross section ($s = m_V^2$) for the vector meson ϕ or ω, δ_ϕ is a relative phase of $\phi-\omega$ mixing, A_{bg} is the non-resonant part of the cross section, $F_{3\pi}(s)$ is a smooth function which describes the dynamics of $\phi(\omega) \to 3\pi$ decay including the phase space. Non-resonant

Table 2: Reconstruction efficiencies and measured 3π cross section

$2E,\ MeV$	$\int Ldt, nb^{-1}$	$N_{3\pi}$	δ_{MC}	δ_{rad}	δ_{wid}	$\sigma_{3\pi}, nb$
994.00 ± 0.20	152.04 ± 0.70	96 ± 12	0.15 ± 0.06	-0.136	0	18 ± 3
1012.76 ± 0.06	110.90 ± 0.58	376 ± 21	0.15 ± 0.06	-0.239	0.006	108 ± 10
1016.54 ± 0.07	85.47 ± 0.51	796 ± 30	0.13 ± 0.07	-0.278	0.015	298 ± 16
1018.26 ± 0.06	93.50 ± 0.54	1379 ± 40	0.20 ± 0.05	-0.284	-0.010	533 ± 23
1018.87 ± 0.06	110.79 ± 0.58	1917 ± 48	0.23 ± 0.04	-0.276	-0.028	650 ± 25
1019.51 ± 0.06	82.96 ± 0.49	1615 ± 43	0.13 ± 0.04	-0.254	-0.031	627 ± 21
1020.76 ± 0.06	89.12 ± 0.51	1276 ± 39	0.06 ± 0.05	-0.162	0.004	369 ± 16
1021.35 ± 0.06	80.80 ± 0.52	867 ± 32	0.09 ± 0.06	-0.105	0.013	265 ± 16
1021.54 ± 0.06	85.50 ± 0.50	828 ± 31	0.23 ± 0.06	-0.084	0.014	274 ± 18
1022.23 ± 0.06	93.42 ± 0.53	644 ± 28	0.15 ± 0.06	0.004	0.015	164 ± 16
1022.94 ± 0.06	123.36 ± 0.62	584 ± 27	0.15 ± 0.06	0.104	0.013	103 ± 11
1025.35 ± 0.07	114.33 ± 0.59	281 ± 19	0.15 ± 0.06	0.600	0.006	37 ± 6
1029.20 ± 0.07	121.73 ± 0.63	110 ± 14	0.15 ± 0.06	2.170	0.003	7 ± 4
1040.00 ± 0.20	81.76 ± 0.51	25 ± 9	0.15 ± 0.06	56.588	0	$0.1^{+4}_{-0.1}$

background can originate either from the higher resonances such as $\omega(1400)$ or the existence of non-resonant diagrams like box anomalies [17].

The energy dependence of the ϕ-meson width was written as

$$\Gamma_\phi(s) = \Gamma_\phi \left(B_{K^+K^-} \frac{m_\phi^2 F_{K^+K^-}(s)}{s F_{K^+K^-}(m_\phi^2)} + B_{K_SK_L} \frac{m_\phi^2 F_{K_SK_L}(s)}{s F_{K_SK_L}(m_\phi^2)} + \right.$$
$$\left. + B_{\eta\gamma} \frac{F_{\eta\gamma}(s)}{F_{\eta\gamma}(m_\phi^2)} + B_{3\pi} \frac{\sqrt{s} F_{3\pi}(s)}{m_\phi F_{3\pi}(m_\phi^2)} \right), \quad (9)$$

and the ω-meson width

$$\Gamma_\omega(s) = \Gamma_\omega \cdot \left(B_{\pi^+\pi^-} \frac{m_\omega^2 F_{2\pi}(s)}{s F_{2\pi}(m_\omega^2)} + B_{\pi^0\gamma} \frac{F_{\pi^0\gamma}(s)}{F_{\pi^0\gamma}(m_\omega^2)} + B_{3\pi} \frac{\sqrt{s} F_{3\pi}(s)}{m_\omega F_{3\pi}(m_\omega^2)} \right), \quad (10)$$

where

$$F_{K\bar{K}}(s) = (s/4 - m_K^2)^{3/2}, F_{\eta\gamma}(s) = (\sqrt{s}(1 - m_\eta^2/s))^3. \quad (11)$$

The cross section values were fitted by the function (6). For the $F_{3\pi}(s)$ calculation the model assuming the decay $\phi(\omega) \to \rho\pi \to 3\pi$ was used. The

ϕ-meson mass, peak cross section and background cross section were optimized, while Γ_ϕ and ω-meson parameters were fixed at their world average values [15]. The following results were obtained:

$$m_\phi = 1019.51 \pm 0.07 \pm 0.10\ MeV,$$
$$\delta_{\phi-\omega} = 162 \pm 17^\circ,$$
$$\sigma_{peak} = 619 \pm 39 \pm 12\ nb,$$
$$\sigma_{bg} = 0.32 \pm 0.22\ nb,$$
$$\chi^2/N_f = 11/10.$$

The experimental points and the fitting curve are shown in Fig. 2. The second error for m_ϕ characterizes the uncertainty of the collider energy. If Γ_ϕ

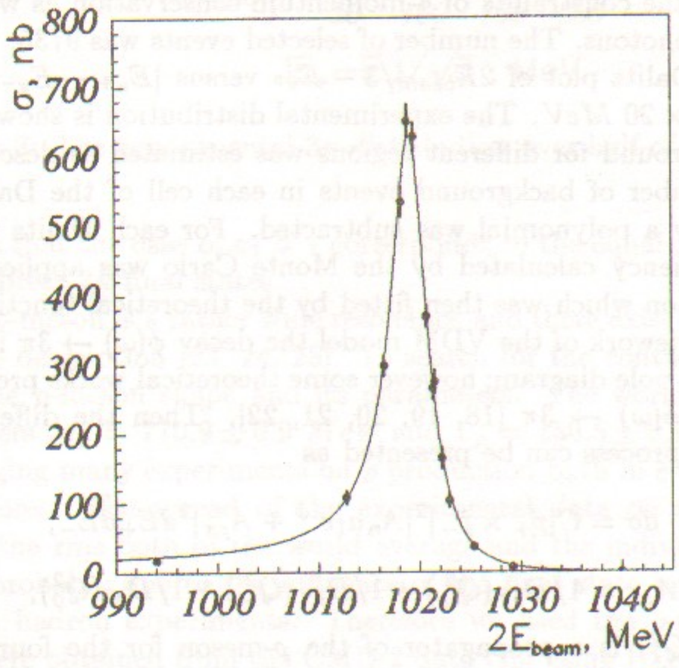

Figure 2: The excitation curve for the ϕ-meson in the channel $\pi^+\pi^-\pi^0$.

is free, its optimal value is 4.21 ± 0.13 MeV which doesn't contradict to [15]. Other parameters do not change considerably, but the accuracy of the phase

determination $\delta_{\phi-\omega} = 161 \pm 25°$ becomes worse. The obtained data on the width and peak cross section correspond to the following branching ratio of $\phi \to 3\pi$ if the value $\Gamma_{ee}/\Gamma_{total} = (3.00 \pm 0.06) \times 10^{-4}$ [15] is used:

$$B_{\phi\to 3\pi} = 0.145 \pm 0.009 \pm 0.003,$$

where the first error is statistical and the second one is systematic and related to the efficiency determination.

These values are consistent with the corresponding world average values.

Dalitz plot analysis

To study the $\phi \to 3\pi$ decay dynamics, the Dalitz plot was analyzed. Reconstructed events from 8 energy points in the range of $1016 - 1023\ MeV$ were selected for the plot. The pion momentum values used in this analysis were calculated by the kinematic reconstruction using the maximum likelihood method with the constraints of 4-momentum conservation as well as the π^0 origin of two photons. The number of selected events was 9735. We used the symmetrical Dalitz plot of $2E_{beam}/3 - E_{\pi^0}$ versus $|E_{\pi+} - E_{\pi-}|/\sqrt{3}$ with a bin size of $20 \times 20\ MeV$. The experimental distribution is shown in Fig. 3.

The background for different regions was estimated as described above. Then the number of background events in each cell of the Dalitz plot approximated by a polynomial was subtracted. For each Dalitz plot cell the detection efficiency calculated by the Monte Carlo was applied to get the final distribution which was then fitted by the theoretical function.

In the framework of the VDM model the decay $\phi(\omega) \to 3\pi$ is dominated by the $\phi(\omega)\rho\pi$ pole diagram; however some theoretical works predict a direct contact term $\phi(\omega) \to 3\pi$ [18, 19, 20, 21, 22]. Then the differential cross section of the process can be presented as

$$d\sigma = C|\vec{p}_+ \times \vec{p}_-|^2 |A_n a_1 e^{i\varphi} + A_{\rho\pi}|^2 dE_+ dE_-, \qquad (12)$$

$$A_{\rho\pi} = 1/D_{\rho+}(Q_+^2) + 1/D_{\rho-}(Q_-^2) + 1/D_{\rho^0}(Q_0^2), \qquad (13)$$

where $1/D_{\rho^i}(Q_i^2)$ is a propagator of the ρ-meson for the four-momentum squared Q_i^2; $A_n a_1 e^{i\varphi}$ is the contact term amplitude; C is a normalization constant(which depends on s). Another normalization constant, $(A_n = 7.92)$, is defined by the condition:

$$\int |\vec{p}_+ \times \vec{p}_-|^2 |A_n|^2 dE_+ dE_- = \int |\vec{p}_+ \times \vec{p}_-|^2 |A_{\rho\pi}|^2 dE_+ dE_-.$$

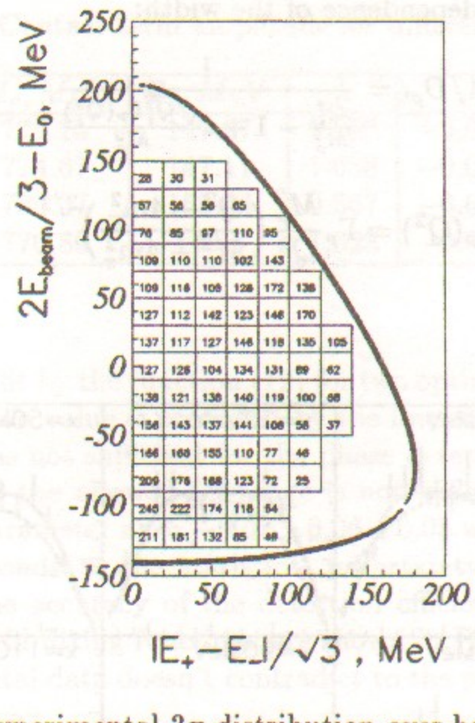

Figure 3: The experimental 3π distribution over half of the Dalitz plot.

It means that the case of $a_1 = 1$ corresponds to the equal contributions from $\rho\pi$ and direct 3π final states.

The ρ-meson is a rather wide resonance and there exist various models for its shape description [23, 24, 25]. To search for the contact term we should define the ρ-meson shape and its parameters. The world average ρ-meson parameters $M_\rho = 770.9 \pm 0.9\ MeV$ and $\Gamma_\rho = 150.5 \pm 0.9\ MeV$ are results of averaging many experiments on ρ production both in e^+e^- and in hadron interactions. The spread of the experimental data on the ρ-meson mass exceeds the rms both of the world average and the individual experiments. This is probably due to the influence of the final state interaction on the ρ shape in hadron experiments. Therefore we used the ρ-meson parameters which were obtained from the CMD-2 data [26] using HLS model [27]($M_\rho = 775.1 \pm 0.7\ MeV$ and $\Gamma_\rho = 147.9 \pm 1.5\ MeV$) and are in good agreement with the previous e^+e^- measurements at VEPP-2M [28]. The charged ρ-meson parameters have been measured recently in $\tau \to \rho\nu$ [29] and are also in good agreement with those of the ρ^0 from e^+e^- data [26].

The shape of the ρ-meson was described by the relativistic Breit-Wigner

with the following Q^2 dependence of the width:

$$1/D_{\rho'} = \frac{1}{\frac{Q_i^2}{M_\rho^2} - 1 + i\frac{\sqrt{Q_i^2}\Gamma_\rho(Q_i^2)}{M_\rho^2}},$$

$$\Gamma_\rho(Q^2) = \Gamma_\rho \frac{M_\rho^2}{Q^2}\Big(\frac{Q^2 - 4m_\pi^2}{M_\rho^2 - 4m_\pi^2}\Big)^{3/2}.$$

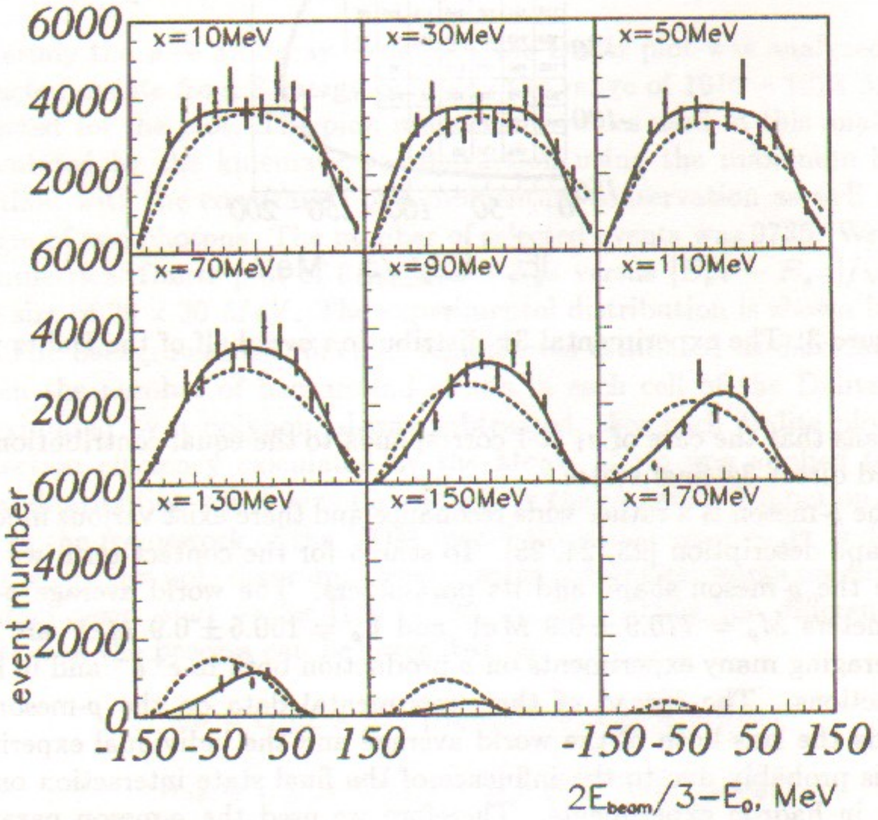

Figure 4: Dynamics of the 3π-decay.
Each plot is a slice of the two dimensional Dalitz plot along the axis $Y = 2E_{beam} - E_{\pi^0}$ for a certain bin of $X = |E_+ - E_-|/\sqrt{3}$ of 20 MeV width. The fitted functions are: solid line – optimal a_1 (which is indistinguishable from pure $\rho\pi$); dashed line – only contact term without $\rho\pi$.

Table 3: Contact term amplitude for different models of ρ

Model [24]	M_ρ, MeV	Γ_ρ, MeV	λ	a_1	χ^2/N_f
HLS	775.15	147.67	1.056	-0.020 ± 0.050	84/77
VDM1	774.67	147.11	1.038	-0.013 ± 0.051	83/77
VDM2	780.37	155.44	0.567	-0.038 ± 0.053	89/77
WCCWZ	770.89	140.6	1.623	-0.022 ± 0.047	82/77

The data were fit by the function (12) for two optimized parameters C, a_1. We used a fixed zero value φ predicted by the low energy theorem [18]. The existing accuracy is not sufficient for the phase determination because the ρ width is large and the allowed Q^2-range is not wide enough. The fit gives the value of the parameter $a_1 = -0.01 \pm 0.06 \pm 0.05$ with $\chi^2/N_f = 1.08$. The first error corresponds to the statistical uncertainty while the second one appears due to the accuracy of the detection efficiency. The experimental points together with fitting functions are shown in Fig. 4.

The experimental data doesn't contradict to the pure $\phi \to \rho\pi$ mechanism to describe the decay.

As mentioned above, the value of a_1 depends on the ρ-meson shape. To estimate the error caused by the model uncertainty we tried several models which describe $e^+e^- \to \pi^+\pi^-$ data [24]. The results are presented in Table 3. The parameter λ is a fitting parameter describing the ρ width energy dependence in the models [24].

$$\Gamma_\rho(Q^2) = \Gamma_\rho\Big(\frac{M_\rho^2}{Q^2}\Big)^{(\lambda+1)/2}\Big(\frac{Q^2 - 4m_\pi^2}{M_\rho^2 - 4m_\pi^2}\Big)^{3/2}.$$

Taking into account the model dependence, we can set limits on the contact term amplitude at 90% C.L.:

$$-0.16 < a_1 < 0.11$$

That doesn't contradict to the result of [7] $\Gamma_{\phi\to\rho\pi}/\Gamma_{\phi\to 3\pi} > 0.8$ at 90% C.L., where the interference of the $\rho\pi$-amplitude and the contact term was ignored.

The contribution of the contact term can not be described as a branching ratio of the direct $\phi \to 3\pi$ decay since the cross section (12) contains a strong interference term $2\int C|\vec{p}_+ \times \vec{p}_-|^2|A_n a_1 e^{i\varphi} A_{\rho\pi}|^2 dE_+ dE_-$ due to the large width of ρ-meson. It means that the $\phi \to 3\pi$ decay has to be characterized

by the branching ratio which includes both final states and by the contact term contribution a_1 relatively to the amplitude of $\phi \to \rho\pi$.

Theoretical predictions for this quantity also show a spread of values. For example, the value of the contact term predicted in [20] is expressed via the ρ coupling constant $g_{\rho\pi\pi}$:

$$A_n a_1 = -\frac{1-3\alpha}{\alpha},$$

where $\alpha = (\frac{f_\pi g_{\rho\pi\pi}}{M_\rho})^2 \approx 0.55$, for $f_\pi \approx 93\ MeV$ and $\frac{g^2_{\rho\pi\pi}}{4\pi} \approx 3$. It corresponds to $a_1 \approx 0.15$. According to [19] the contact term should be

$$A_n a_1 = -\frac{1-3\alpha+3/2\alpha^2}{\alpha},$$

corresponding to $a_1 \approx 0.05$. Unfortunately, the present accuracy is not sufficient to confirm or reject these predictions.

It should also be mentioned that there is a model [30] which predicts an interaction between a pion and ρ in the final state which can change relative phases and amplitudes of $\rho\pi$-terms in (13), but its effect is small and beyond the present experimental accuracy.

Search for direct decay $\phi \to \pi^+\pi^-\gamma\gamma$

The decay of the ϕ-meson to the final state with two pions and two photons can contain a small admixture of the non $\phi \to \pi^+\pi^-\pi^0$ mode as, for example, $\phi \to \gamma\eta \to \pi^+\pi^-\gamma\gamma$. In the present work we searched for events of the $\phi \to \pi^+\pi^-\gamma\gamma$ when there is no intermediate π^0 or $\eta \to \pi\pi\gamma$ state.

For this purpose we selected events with two photons and two tracks satisfying the requirements described earlier, but with a stronger cut for $R_{min} < 0.2\ cm$. To suppress the $e^+e^-\gamma\gamma$ background the energy deposition in the calorimeter for each charged particle was required to be different from its momentum $|E_{ch\ i}/p_i - 1| > 0.2$. The detected photon was required to have a polar angle within the region of the good efficiency of the calorimeter $|\theta_\gamma - \pi/2| < 0.67$ and the detected photon energy $E_\gamma > 30\ MeV$. It was also required that the photon lies more than 0.5 radians away from the closest charge particle cluster: $\Delta\psi_{\gamma ch_i} > 0.5$ to suppress the fake clusters produced by a pion shower.

The nonresonant background for this process coming from radiative processes $e^+e^- \to e^+e^-\gamma\gamma$, $e^+e^- \to \rho\gamma\gamma$ and $e^+e^- \to \rho\gamma$ was estimated from the

analysis of the cross section energy dependence. The contribution of the resonant background due to the wrong reconstruction of the decays $\phi \to K\bar{K}$ and $\phi \to \eta\gamma$ was suppressed by applying a cut $\chi^2 < 5$.

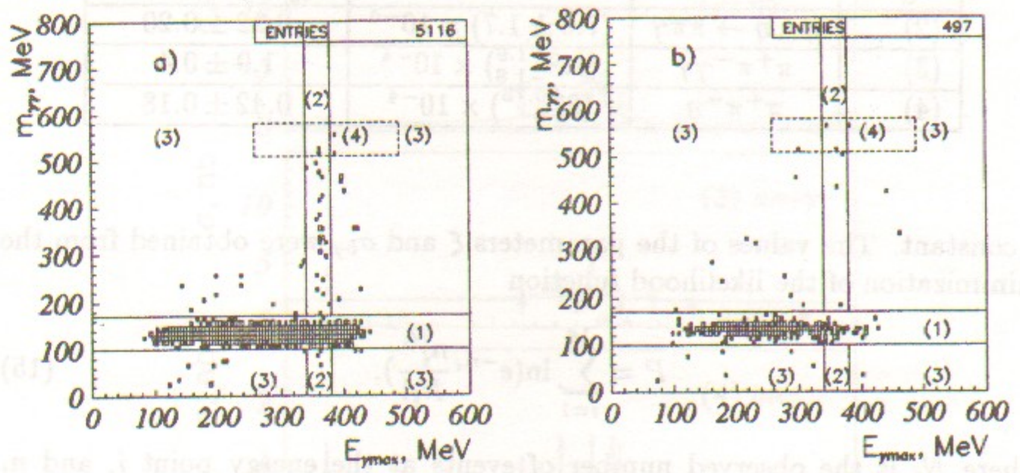

Figure 5: Scatter plot of two photon invariant mass versus maximum photon energy: a) – for resonance region; b) – for background.

In Fig. 5 the distributions of $m_{\gamma\gamma}$ versus $E_{\gamma max}$ for selected events are shown for the resonance energy region $1015 < E_{c.m.} < 1025\ MeV$ and outside it. The regions in Fig. 5 correspond to the following processes:

- (1) $100 < m_{\gamma\gamma} < 170\ MeV$ – 3π-events;
- (2) $|m_{\gamma\gamma} - 135| > 35\ MeV$ and $340 < E_{\gamma max} < 380\ MeV$ – $\phi \to \gamma\eta \to \pi^+\pi^-\gamma\gamma$;
- (3) $|m_{\gamma\gamma} - 135| > 35\ MeV$, $|E_{\gamma max} - 360| > 20\ MeV$ and $E_{\gamma max} > 70\ MeV$ – the searched process $\phi \to \rho\gamma\gamma$;
- (4) $590 > m_{\gamma\gamma} > 510\ MeV$ – G-parity forbidden process $\phi \to \pi^+\pi^-\eta$, $\eta \to \gamma\gamma$.

52 and 8 events were found in regions (3) and (4) respectively at 14 energy points. The average number of events at each energy point was written as

$$n_i = (\sigma_{bg} + \xi\sigma_{res}(s))L, \qquad (14)$$

where $\sigma_{res}(s)$ is the resonant cross section which was assumed to have the same shape as for 3π (6) and σ_{bg} is a background cross section taken to be

Table 4: Branching ratios and background cross sections for the processes

region	reaction	Br_i	$\sigma'_{bg} = \sigma_{bg}/\xi_1$, nb
(2)	$\eta\gamma, \eta \to \pi\pi\gamma$	$(7.6 \pm 1.7) \times 10^{-4}$	0.22 ± 0.20
(3)	$\pi^+\pi^-\gamma\gamma$	$(1.8^{+1.9}_{-1.8}) \times 10^{-4}$	1.9 ± 0.4
(4)	$\pi^+\pi^-\eta$	$(0^{+0.73}_{-0}) \times 10^{-4}$	0.42 ± 0.18

a constant. The values of the parameters ξ and σ_{bg} were obtained from the minimization of the likelihood function

$$P = \sum_{i=1}^{14} \ln(e^{-n_i} \frac{n_i^{N_i}}{N_i!}), \tag{15}$$

where N_i is the observed number of events at the energy point i, and n_i is the expected number which depends on ξ and σ_{bg} (14). According to the Monte Carlo simulation the detection efficiency of $\phi \to \eta\pi^+\pi^-$ is the same as for 3π with 10% accuracy. Assuming the detection efficiency of the $\pi\pi\gamma\gamma$ to be the same as for the 3π-reaction, we can estimate the branching ratio $Br(\phi \to \pi\pi\gamma\gamma) = \xi_3/\xi_1 Br(\phi \to 3\pi)$, and $Br(\phi \to \pi^+\pi^-\eta, \eta \to \gamma\gamma) = \xi_4/\xi_1 Br(\phi \to 3\pi)$, where ξ_1, ξ_3, ξ_4 are the obtained values of the parameter ξ for the regions (1), (3) and (4) respectively. Figure 6 shows the cross sections for three regions (2-4). The optimal values of the branching ratios and background cross sections are shown in Table 4. The obtained value for $Br(\phi \to \eta\gamma)Br(\eta \to \pi^+\pi^-\gamma)$ doesn't contradict to the world average value $(6.2 \pm 0.6) \times 10^{-4}$. The optimal values of $\xi < 0$ for regions (3,4) lie in the unphysical region and we can set upper limits for these processes. The found number of events corresponds to upper limits 5×10^{-4} at 90% C.L. for $\pi^+\pi^-\gamma\gamma$ and 1.2×10^{-4} at 90% C.L. for $\pi^+\pi^-\eta$, $\eta \to \gamma\gamma$. Taking into account the branching ratio of the decay $Br(\eta \to \gamma\gamma) = 39.25 \pm 0.31\%$ we found an upper limit for the process $Br(\phi \to \eta\pi^+\pi^-) < 3 \times 10^{-4}$ at 90 % C.L. It is higher than predicted in [31]. If the observed events in $\pi^+\pi^-\gamma\gamma$ are interpreted as those of the process $\phi \to \rho\gamma\gamma$ and calculating the efficiency according to [32], we can set an upper limit for the process $Br(\phi \to \rho\gamma\gamma) < 5 \times 10^{-4}$ at 90 % C.L.

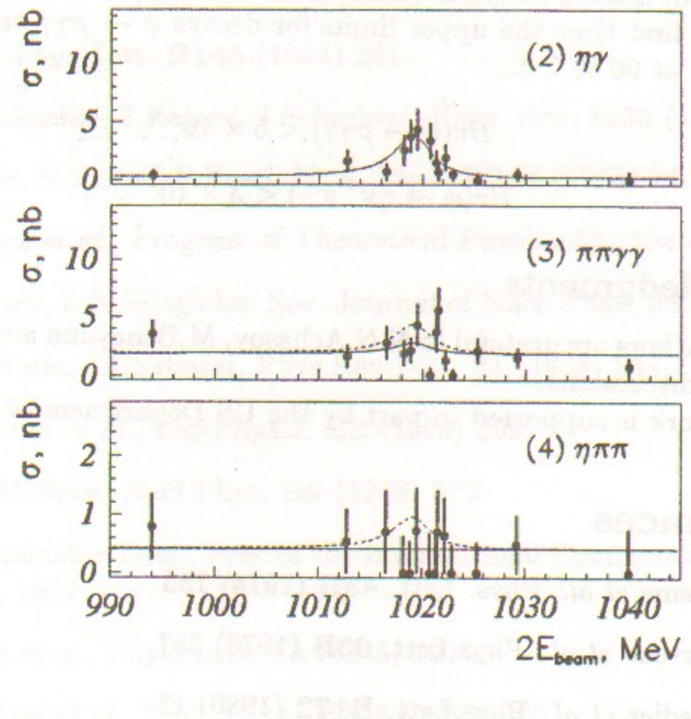

Figure 6: Cross section behaviour for the $\pi\pi\gamma\gamma$ final state for regions of Fig. 5. Solid and dashed lines correspond to the optimal fit parameters and 90% C.L. upper limits respectively.

Conclusions

Using the data sample of 11169 completely reconstructed $\pi^+\pi^-\pi^0$ events collected by CMD-2, we have obtained the following results. The branching ratio of $\phi \to \pi^+\pi^-\pi^0$ and the angle of $\phi - \omega$ mixing were measured to be

$$\sigma_{peak} = 619 \pm 39 \pm 12\ nb,$$

$$B_{\phi \to 3\pi} = 0.145 \pm 0.009 \pm 0.003,$$

$$\delta_{\phi-\omega} = 162 \pm 17^\circ.$$

The distribution of 9735 $\phi \to 3\pi$ events on the Dalitz plot was analyzed and it was found that the mechanism of the decay is consistent with the $\rho\pi$ model. The possible contribution of the contact term amplitude is

$$-0.16 < a_1 < 0.11$$

at 90 % C.L. if the ρ shape is taken from e^+e^- data.

For the first time the upper limits for decays $\phi \to \rho\gamma\gamma$ and $\phi \to \eta\pi^+\pi^-$ were found at 90 % C.L.:

$$Br(\phi \to \rho\gamma\gamma) < 5 \times 10^{-4},$$

$$Br(\phi \to \eta\pi^+\pi^-) < 3 \times 10^{-4}.$$

Acknowledgments

The authors are grateful to N.N.Achasov, M.Benayoun and Z.K.Silagadze for useful discussions.

This work is supported in part by the US Department of Energy.

References

[1] G.Cosme *et al.*, Phys. Lett. **48B** (1974) 155.

[2] G.Parrour *et al.*, Phys.Lett. **63B** (1976) 357.

[3] A.Cordier *et al.*, Phys.Lett. **B172** (1980) 13.

[4] A.D.Bukin *et al.*, Sov. Journal of Nucl. Phys. **27** (1978) 516.

[5] L.M.Kurdadze *et al.*, Preprint INP **84-07**, Novosibirsk, 1984.

[6] S.I.Dolinsky *et al.*, Phys. Rep. **202** (1991)99.

[7] G.Parrour *et al.*, Phys.Lett. **63B** (1976) 362.

[8] G.A.Aksenov *et al.*, Preprint Budker INP **85-118**, Novosibirsk, 1985.

[9] E.V.Anashkin *et al.*, ICFA Instrumentation Bulletin **5** (1988) 18.

[10] V.V.Anashin *et al.*, Preprint INP **84-114**, Novosibirsk, 1984.

[11] E.V.Anashkin *et al.*, NIM **A283** (1989) 752.

[12] V.M.Aulchenko *et al.*, NIM **A336** (1993) 53.

[13] R.R.Akhmetshin *et al.*, Phys. Lett. **B364** (1995) 199.

[14] E.V.Anashkin *et al.*, NIM **A323** (1992) 178.

[15] R.M.Barnett *et al.*, Phys. Rev. **D54** (1996) 1.

[16] E.A.Kuraev, V.S.Fadin, Sov. Journal of Nucl. Phys. **41** (1985) 466.

[17] M.Benayoun *et al.*, Z.Phys. **C58** (1993) 31, **C65** (1995) 399.

[18] S.Rudaz, Phys.Lett. **B145** (1984) 281.

[19] Ö.Kaymakcalan, S.Rajeev, J.Schechter, Phys. Rev. **D30** (1984) 594.

[20] Y.Brihaye, N.K.Pak, P.Rossi, Nucl. Phys. **B254** (1985) 71.

[21] T.Fujiwara *et al.*, Progress of Theoretical Physics **73** (1985) 926.

[22] E.A.Kuraev, Z.K.Silagadze, Sov. Journal of Nucl. Phys. **58** (1995) 1687.

[23] G.J.Gounaris, J.J.Sakurai, Phys.Rev.Lett. **21** (1968) 244.

[24] M.Benayoun *et al.*, Eur.Phys.J. **C2** (1998) 269.

[25] J.Pisut, M.Roos, Nucl.Phys. **B6** (1968) 325.

[26] R.R.Akhmetshin *et al.*, Proc.of the International Conference HADRON-97, BNL, 1997.

[27] M.Bando *et al.*, Phys. Lett. **54** (1985) 1215.

[28] L.M.Barkov *et al.*, Nucl. Phys. **B256** (1985) 365.

[29] R.Barate *et al.*, Z.Phys. **C76** (1997) 15.

[30] N.N.Achasov, A.A.Kozhevnikov, Phys.Rev.**D49** (1994) 5773.

[31] V.A.Karnakov, Sov. Journal of Nucl. Phys. **42** (1985) 634.

[32] Pyungwon Ko, Jungil Lee, H.S.Song, Phys. Lett. **B366** (1996) 287.

R.R.Akhmetshin, G.A.Aksenov, E.V.Anashkin, M.Arpagaus, B.O.Baibusinov, V.S.Banzarov, L.M.Barkov, A.E.Bondar, D.H.Brown, D.V.Chernyak, V.V.Danilov, A.S.Dvoretsky, S.I.Eidelman, G.V.Fedotovich, N.I.Gabyshev, A.A.Grebeniuk, D.N.Grigoriev, V.W.Hughes, P.M.Ivanov, B.I.Khazin, I.A.Koop, L.M.Kurdadze, A.S.Kuzmin, I.B.Logashenko, P.A.Lukin, Yu.I.Merzlyakov, I.N.Nesterenko, V.S.Okhapkin, A.A.Polunin, V.I.Ptitzyn, T.A.Purlatz, B.L.Roberts, N.I.Root, A.A.Ruban, N.M.Ryskulov, A.G.Shamov, Yu.M.Shatunov, B.A.Shwartz, V.A.Sidorov, A.N.Skrinsky, V.P.Smakhtin, I.G.Snopkov, E.P.Solodov, P.Yu.Stepanov, A.I.Sukhanov, V.M.Titov, J.A.Thompson, Yu.V.Yudin, S.G.Zverev.

Study of dynamics of $\phi \to \pi^+\pi^-\pi^0$ decay with CMD-2 detector

Budker INP 98-30

Ответственный за выпуск А.М. Кудрявцев
Работа поступила 23.06.1998 г.

Сдано в набор 24.06.1998 г.
Подписано в печать 24.06.1998 г.
Формат бумаги 60×90 1/16 Объем 1.4 печ.л., 1.1 уч.-изд.л.
Тираж 200 экз. Бесплатно. Заказ № 30

Обработано на IBM PC и отпечатано на
ротапринте ИЯФ им. Г.И. Будкера СО РАН
Новосибирск, 630090, пр. академика Лаврентьева, 11.